

Chain length dependence of liquid–liquid equilibria of binary polymer solutions

Bong Ho Chang, Kyong-Ok Ryu and Young Chan Bae*

School of Chemical Engineering, Hanyang University, Seoul 133-791, Korea

(Received 3 June 1997)

The proposed model in our previous study¹ improves the mathematical approximation defect and gives a new expression for the configurational energy of mixing using the fractional form rather than the algebraic form with second-order approximation for the configurational energy of non-random mixing². In this study, we introduce new universal constants to take into account the chain length dependence of a polymer in a solvent. Our proposed model shows a slight discrepancy when compared with experimental data and gives a better understanding of phase equilibria dependence on the chain length of the polymer. © 1997 Elsevier Science Ltd. All rights reserved.

(Keywords: liquid–liquid equilibria; non-random mixing; chain length dependence)

INTRODUCTION

The lattice model is a starting point for the prediction of liquid–liquid equilibria in polymer solutions. However, a variety of polymer–solution theories have been developed during the last half-century. Molecular-based thermodynamic models for describing liquid–liquid equilibria in polymer mixtures can be divided into four categories, each corresponding to a particular statistical mechanical framework: incompressible-lattice models, generalized van der Waals partition-function theories, compressible-lattice models^{3–6}, and off-lattice (continuous-space) models of chain fluids.

The most widely used and best known of the incompressible-lattice models is the Flory–Huggins theory^{7–11} which illustrates in a simple way the competition between the entropy of mixing and the attractive forces that produces liquid–liquid phase separation at low temperatures with an upper critical solution temperature. Many theoretical improvements, including Guggenheim's quasi-chemical model¹², have been made by various workers, include chain connectivity and non-random mixing¹². In addition, the Flory–Huggins model and the quasi-chemical model give too narrow or parabolic liquid–liquid coexistence curves near the critical region when compared with experimental data in which the interaction parameter is assumed to be only inversely proportional to temperature. It ignores its composition dependence. Extensive experimental results by many researchers clearly show, however, that the interaction parameter is a function of both polymer concentration and temperature for most polymer-containing systems and its temperature dependence is not a simple proportionality to the inverse temperature.

Furthermore, to pursue a formal 'exact' solution to the lattice model using advanced statistical-mechanical methods^{13–20}, Freed and co-workers developed a lattice field theory (or lattice cluster theory)^{13–20} for polymer/solvent systems which is formally an exact mathematical solution of the Flory–Huggins model. In this theory, they

have developed the first completely exact and systematic analysis of the macromolecular lattice models. Instead of the usual approximate counting of microstates, Freed's technique begins with a rigorous formulation of the partition function of the lattice and expands the Helmholtz free energy as a series of integrals. The terms can then be grouped to provide an expansion in the reciprocal of the lattice coordination number z . The effects of nearest-neighbour interactions are evaluated via a perturbation expansion in the interaction energies whose individual coefficients are represented in similar fashion and further expanded in the power of z^{-1} . The technical complexity of the calculation dictates that only a few lower-order terms in this secondary expansion can be evaluated. The terms that are zeroth order in z^{-1} correspond to the limit of infinite coordination number. For practical reasons, the infinite series with respect to coordination number, temperature, and composition in this theory are truncated at a certain order. Therefore, this theory still remains deficient for the correlation of liquid–liquid equilibria.

Recently, Lambert *et al.*²¹ reported a new expression for $\Delta_{\text{mix}}A$ for incompressible monomer/ r -mer mixtures obtained by correlating the Monte-Carlo simulation results. In their study, they used the algebraic form, which is a Redlich–Kister expansion² truncated after the third term, to correlate energy of mixing data with Monte-Carlo simulation results. They introduce chain length dependent parameters using the simulation results.

Bae²² reported a modified version of the extended Flory–Huggins equation being applicable to represent the chain length dependence of liquid–liquid equilibria for some binary polymer solutions by adding the chain length dependence term in the interaction parameter. These improvements provide better agreement with experimental data by widening the liquid–liquid coexistence curve. The purpose of this study is to improve the discrepancy in predicting the phase equilibria behaviour of binary polymer solutions by taking the chain length dependence of the polymer into account for our previously proposed model¹ in which only universal parameters are used. The coexistence curves generated by the previous model and the model

* To whom correspondence should be addressed

adding the chain length dependence term are compared with experimental data.

MODEL DEVELOPMENT

Internal and Helmholtz energies of mixing

The description of the lattice model starts with a simple cubic lattice (coordination number, $z = 6$) containing N_r sites. The lattice is filled completely by N_1 molecules of type 1, which occupy only one lattice site ($r_1 = 1$), and N_2 molecules of type 2, which occupy r_2 nearest-neighbour lattice sites (r -mer). The energy of mixing is related to the number of nearest-neighbour pairs²³ by

$$\frac{\Delta_{\text{mix}}U}{N_r\varepsilon} = \frac{1}{2} \frac{N_{12}}{N_r} \quad (1)$$

where N_{12} related to the total number of contacts of component i (zq_iN_i) is the total number of 1-2 pairs and ε is the interchange energy as defined by

$$\varepsilon = \varepsilon_{11} + \varepsilon_{22} - 2\varepsilon_{12} \quad (2)$$

where ε_{ij} is the i - j nearest-neighbour interaction energy. The Helmholtz energy of mixing ($\Delta_{\text{mix}}A$) is obtained by integrating the Gibbs-Helmholtz equation using Guggenheim's athermal entropy of mixing as the boundary condition:

$$\frac{\Delta_{\text{mix}}A}{N_r kT} = \left(\frac{\Delta_{\text{mix}}A}{N_r kT} \right)_{1/\tilde{T}=0} + \int_0^{1/\tilde{T}} \frac{\Delta_{\text{mix}}U}{N_r \varepsilon} d\left(\frac{1}{\tilde{T}}\right) \quad (3)$$

$$\left(\frac{\Delta_{\text{mix}}A}{N_r kT} \right)_{1/\tilde{T}=0} = \frac{\phi_1}{r_1} \ln \phi_1 + \frac{\phi_2}{r_2} \ln \phi_2 + \frac{z}{2} \left[\phi_1 \frac{q_1}{r_1} \ln \frac{\theta_1}{\phi_1} + \phi_2 \frac{q_2}{r_2} \ln \frac{\theta_2}{\phi_2} \right] \quad (4)$$

A dimensionless temperature is defined by $\tilde{T} = kT/\varepsilon$, where T is the absolute temperature and k is Boltzmann's constant. r_i , ϕ_i , and θ_i are the number of segments per molecule, volume fraction, and surface fraction of component i , respectively. ϕ_i , and θ_i are defined by:

$$\phi_i = \frac{N_i r_i}{N_1 r_1 + N_2 r_2} \quad (5)$$

$$\theta_i = \frac{N_i q_i}{N_1 q_1 + N_2 q_2} \quad (6)$$

where q_i is the surface area parameter;

$$zq_i = r_i(z-2) + 2 \quad (7)$$

Correlation of simulation data

The fractional form to improve the mathematical approximation and to correlate energy of mixing data to that of the Monte-Carlo simulation²¹ is given by

$$\frac{2\Delta_{\text{mix}}U}{N_r \varepsilon} = \phi_1 \phi_2 \left[\frac{B'}{1 - A'(\phi_2 - \phi_1)} \right] \quad (8)$$

where

$$A' = a_0 + a_1 [\exp(1/\tilde{T}) - 1] \quad (9)$$

$$B' = b_0 + b_1 [\exp(1/\tilde{T}) - 1] \quad (10)$$

where ϕ_1 and ϕ_2 are monomer and r -mer volume fractions, respectively. Parameters A' and B' depend on dimensionless temperature only.

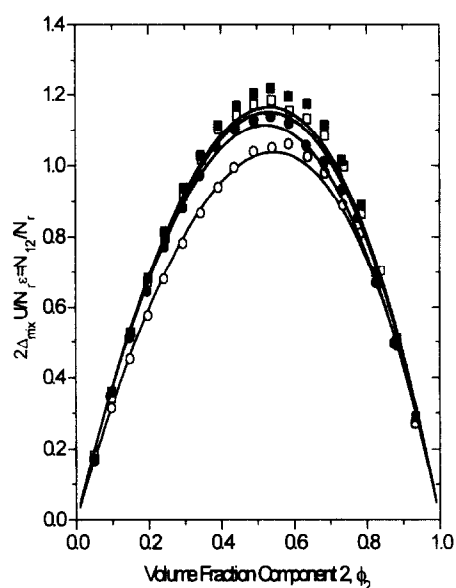


Figure 1 Plots of normalized energy of mixing for monomer (1)/20-mer (2) mixtures as a function of ϕ_2 . Open circles, solid circles, open squares, and solid squares are Monte-Carlo simulation results (Lambert *et al.*²¹) for kT/ε values of 3, 6, 10, and ∞ , respectively. Solid lines are calculated by equation (8)

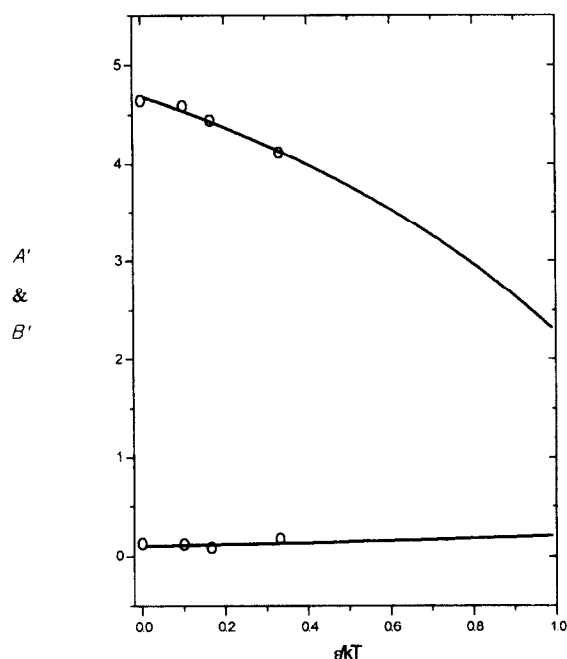


Figure 2 Plots of A' and B' as a function of a reciprocal of dimensionless temperature. The upper solid line is calculated by equation (10). The lower solid line is calculated by equation (9). Open circles are calculated values by correlating with Monte-Carlo simulation results from Lambert *et al.*²¹

Universal constants

Lambert *et al.*²¹ reported that the parameters are very weak functions of r_2 when r_2 is larger than 10. In our previous study, we used the same assumption as Lambert *et al.* Those constants are not adjustable parameters and are determined by comparing with Monte-Carlo simulation results.

Figure 1 shows the energy of mixing for monomer/20-mer ($r_2 = 20$) mixtures as a function of r -mer volume fraction for various dimensionless temperatures. The solid lines are the fit given by equation (8) with best fitting values of a_0 , a_1 , b_0 , and b_1 .

Figure 2 shows A' and B' as a function of reciprocal of dimensionless temperature. The solid lines are given by equations (9) and (10). Our best values obtained for a_0 , a_1 , b_0 , and b_1 are 0.1057, 0.0614, 4.6846, and -1.3970 , respectively.

Chain length dependence term

In our proposed model, parameters a_0 , a_1 , b_0 , and b_1 depend on r -mer chain length. Figure 3 represents the chain length dependence of a_0 , a_1 , b_0 , and b_1 . The parameters appear to be asymptotic values with respect to r_2 . The following equations represent the r -mer dependence of a_0 , a_1 , b_0 , and b_1 :

$$a_0 = 0.00012 + \frac{0.22999(r_2 - 1)}{1 + 1.37129(r_2 - 1)} \quad (11)$$

$$a_1 = -0.01717 + \frac{0.02160(r_2 - 1)}{1 + 0.09642(r_2 - 1)} \quad (12)$$

$$b_0 = 5.79880 - \frac{1.45604(r_2 - 1)}{1 + 1.83417(r_2 - 1)} \quad (13)$$

$$b_1 = -1.42112 - \frac{0.16059(r_2 - 1)}{1 - 1.34296(r_2 - 1)} \quad (14)$$

equations (11)–(14) can be applied to $r_2 \gg 1000$. After $r_2 > 3$, a_0 , a_1 , b_0 , and b_1 are not dependent on r_2 according to Figure 3.

A simple lattice model expression for predicting liquid-liquid equilibria is given by

$$\frac{\Delta_{\text{mix}}A}{N_r kT} = \left(\frac{\Delta_{\text{mix}}A}{N_r kT} \right)_{1/\bar{T}=0} + \frac{1}{2} \phi_1 \phi_2 \left[B \frac{1}{\bar{T}} - \frac{A}{a_1(2\phi_2 - 1)} \ln \left\{ 1 - \frac{a_1(2\phi_2 - 1)}{1 - a_0(2\phi_2 - 1)} \{ \exp(1/\bar{T}) - 1 \} \right\} \right] \quad (15)$$

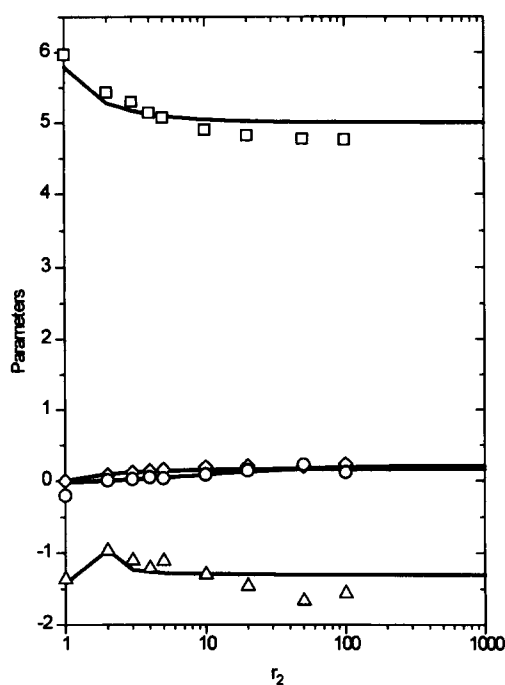


Figure 3 Dependence of parameters a_0 , a_1 , b_0 , and b_1 on r -mer chain length. The squares, diamonds, circles, and triangles calculated by equations (9) and (10) from the simulation results represent b_0 , a_0 , a_1 , and b_1 , respectively. Solid lines are calculated by equations (11)–(14)

$$A = \frac{(a_1 b_0 - a_0 b_1)(2\phi_2 - 1) + b_1}{1 + (a_1 - a_0)(2\phi_2 - 1)} \quad (16)$$

$$B = \frac{b_0 - b_1}{1 + (a_1 - a_0)(2\phi_2 - 1)}$$

and the critical condition is given by

$$\left[\frac{\partial^2 \left(\frac{\Delta_{\text{mix}}A}{N_r kT} \right)}{\partial \phi_1^2} \right]_{T,V} = \left[\frac{\partial^3 \left(\frac{\Delta_{\text{mix}}A}{N_r kT} \right)}{\partial \phi_1^3} \right]_{T,V} = 0 \quad (17)$$

The critical temperature and critical volume fraction can be obtained by solving the following two equations simultaneously:

$$\begin{aligned} & \frac{-1}{1 - \phi_2} + \left(1 - \frac{r_1}{r_2} \right) + \frac{Z}{2} \left[q_1 \left(\frac{\phi_2 - \theta_2}{\phi_2 \phi_1} \right) \right. \\ & \quad \left. + \left(\frac{\theta_1 \theta_2}{\phi_2 \phi_1} - 1 \right) \left(q_1 + q_2 \frac{r_1 \phi_2}{r_2 \phi_1} \right) + q_2 \frac{r_1 (\phi_1 - \theta_1)}{r_2 \phi_1^2} \right] \\ & \quad + 2r_1 \phi_2 Y 2r_1 \phi_2 (2\phi_2 - 1) \left(\frac{\partial Y}{\partial \phi_2} \right) \\ & \quad - r_1 (\phi_2^2 - \phi_2^3) \left(\frac{\partial^2 Y}{\partial \phi_2^2} \right) = 0 \end{aligned} \quad (18)$$

$$\begin{aligned} & \frac{1}{(1 - \phi_2)^2} \\ & \quad + \frac{Z}{2} \left[q_1 \frac{\{ (\phi_2 \phi_1 - \theta_2 \theta_1) - (\phi_2 - \theta_2)(1 - 2\phi_2) \}}{(\phi_2 \phi_1)^2} \right. \\ & \quad \left. + \frac{\theta_1 \theta_2 (\theta_1 - \theta_2 - 1 + 2\phi_2)}{(\phi_2 \phi_1)^2} \left(q_1 + q_2 \frac{r_1 \phi_2}{r_2 \phi_1} \right) \right. \\ & \quad \left. + \left(\frac{\theta_1 \theta_2}{\phi_2 \phi_1} - 1 \right) \left(\frac{r_1 q_2}{r_2 \phi_1^2} \right) + q_2 \frac{r_1 (\phi_2 \phi_1 + \theta_2 \theta_1 - 2\phi_2 \theta_1)}{\phi_2^3 \phi_2} \right] \\ & \quad + 2r_1 Y + 2r_1 (5\phi_2 - 1) \left(\frac{\partial Y}{\partial \phi_2} \right) + r_1 \phi_2 (7\phi_2 - 4) \left(\frac{\partial^2 Y}{\partial \phi_2^2} \right) \\ & \quad - r_1 (\phi_2^2 - \phi_2^3) \left(\frac{\partial^3 Y}{\partial \phi_2^3} \right) = 0 \end{aligned} \quad (19)$$

where

$$Y = \frac{1}{2} \left[B \frac{1}{\bar{T}} - \frac{A}{a_1(2\phi_2 - 1)} \ln \left\{ 1 - \frac{a_1(2\phi_2 - 1)}{1 - a_0(2\phi_2 - 1)} \{ \exp(1/\bar{T}) - 1 \} \right\} \right] \quad (20)$$

The coexistence curve is found from the following conditions:

$$\Delta \mu'_1 = \Delta \mu''_1 \quad (21)$$

$$\Delta \mu'_2 = \Delta \mu''_2 \quad (22)$$

where $\Delta \mu_i$ is the change in chemical potential upon isothermally transferring component i from the pure state to the mixture. Superscripts ' and '' denote two phases at equilibrium. Relative to pure component 1, the chemical potential $\Delta \mu_1$ of component 1 in the solution is defined by

$$\begin{aligned} \Delta\mu_1 &= \left(\frac{\partial \Delta_{\text{mix}} A}{\partial N_1} \right)_{T, N_2} \\ &= \ln(1 - \phi_2) + \phi_2 \left(1 - \frac{r_1}{r_2} \right) + \frac{z}{2} \left[q_1 \ln \frac{\theta_1}{\phi_1} + q_1 (\theta_2 - \phi_2) \right. \\ &\quad \left. + q_2 \frac{r_1 \phi_2}{r_2 \phi_1} (\phi_1 - \theta_1) \right] + r_1 \phi_2^2 Y + r_1 \phi_2^2 \phi_1 \left(\frac{\partial Y}{\partial \phi_1} \right) \end{aligned} \quad (23)$$

and a similar relation holds for $\Delta\mu_2$

$$\begin{aligned} \Delta\mu_2 &= \left(\frac{\partial \Delta_{\text{mix}} A}{\partial N_2} \right)_{T, N_1} \\ &= \ln \phi_2 + (1 - \phi_2) \left(1 - \frac{r_2}{r_1} \right) + \frac{z}{2} \left[q_2 \ln \frac{\theta_2}{\phi_2} + q_2 (\theta_1 - \phi_2) \right. \\ &\quad \left. + q_1 \frac{r_2 \phi_1}{r_1 \phi_2} (\phi_2 - \theta_2) \right] + r_2 \phi_1^2 Y + r_2 \phi_1^2 \phi_2 \left(\frac{\partial Y}{\partial \phi_2} \right) \end{aligned} \quad (24)$$

RESULTS AND DISCUSSION

It is essential to fix model parameters r_2 and ε/k in order to compare calculated results with experimental liquid-liquid equilibria data^{6,24,25}. In this study, to get agreement with the experimental results, r_2 and ε/k are adjusted for all cases from equations (18) and (19), simultaneously. The energy parameter, ε/k , has almost no effect on the shape of the coexistence curve. Therefore, r_2 is the most important parameter to determine the shape of the calculated coexistence curve. According to Figure 3, when r_2 is larger than 3, parameters a_0 , a_1 , b_0 , and b_1 show very small changes. However, these small changes have a very large effect on the shape of the coexistence curve.

Figure 4 shows phase diagrams of poly(isobutylene) (PIB)/diisobutyl ketone systems⁷⁻⁹. Thick solid lines present coexistence curves generated by the model with the chain length dependence term (Case I). Thin solid lines present coexistence curves generated by the model without the chain length dependence term (Case II). As shown in Figure 4, calculated curves from Case I agree very well with experimental data, while Case II predicts narrow coexistence curves. Values of ε/k depend weakly on the chain length of the polymer. ε/k values of Case II for PIB of molecular weight 6 000 000, 285 000, and 22 700 are 68.91, 68.61, 68.59 K, respectively. For Case I, those values are 81.27, 79.99, and 76.66 K, respectively. Our results show that ε/k values of Case I are larger than those of Case II.

The model presented here has considered only liquid-liquid equilibria with an upper critical solution temperature, since it has not considered the oriented intermolecular forces^{25,27,28} and free volume effects³⁻⁶ which are essential for explaining the lower critical solution temperatures²⁹. There is a slight discrepancy between calculated results using Case II and experimental data in the high polymer concentration range. Otherwise, Case II gives a reasonable prediction of critical points. For the high-molecular-weight polymer there is greater deviation between the theoretical prediction and experimental results than for the low-molecular-weight polymer. This is because Case II uses the simulation data for the energy of mixing for monomer/20-mer ($r_2 = 20$) mixtures only. But Case I agrees very well with all the molecular weights of PIB.

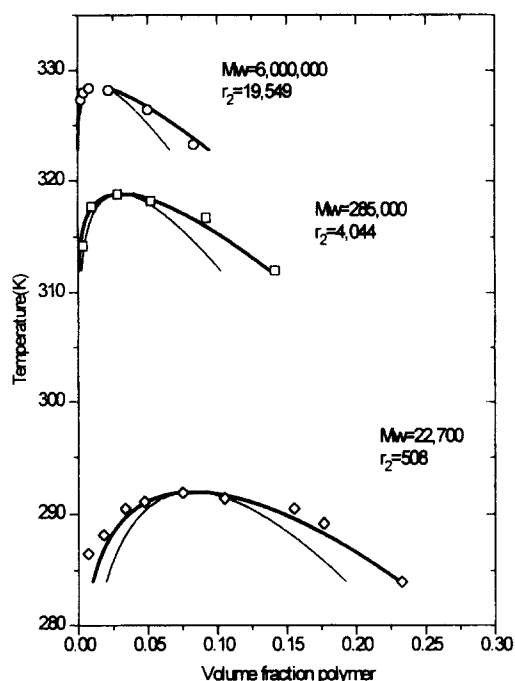


Figure 4 Coexistence curves for PIB/diisobutyl ketone systems. Open diamonds, open squares, and open circles are experimental data (Flory and Shultz²⁶) for PIB of molecular weight 6 000 000, 285 000 and 22 700, respectively. Thick solid lines calculated by equations (17) and (18) (Case I). Thin solid lines are calculated using Case II

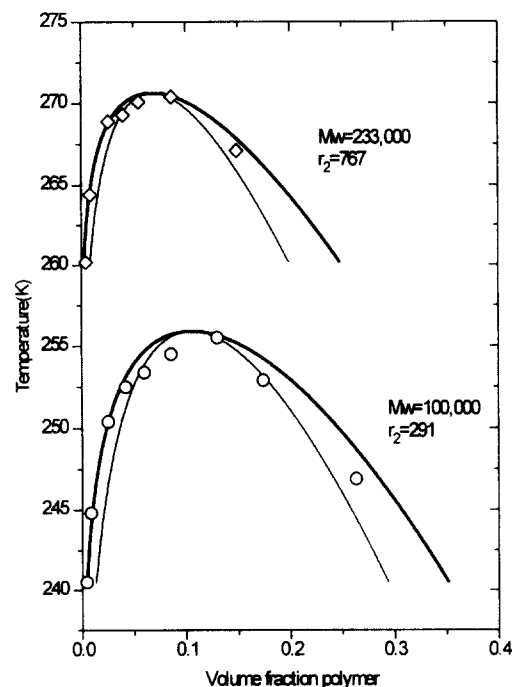


Figure 5 Coexistence curves for PS/*tert*-butyl acetate systems. Open diamonds and circles are experimental data (Bae *et al.*³⁰) for PS of molecular weight 233 000 and 100 000, respectively. Thick solid lines calculated by Case II. Thin solid lines are calculated by Case I

Figure 5 shows phase diagrams of polystyrene (PS)/*tert*-butyl acetate systems^{22,30,31}. ε/k values of Case II for PS of molecular weight 233 000 and 100 000 are 62.04 and 62.68 K, respectively. Those of Case I are 70.15 and 68.68 K, respectively. Similarly, Case I gives a better prediction than that of Case II.

Figure 6 shows a phase diagram of the PS/cyclohexane

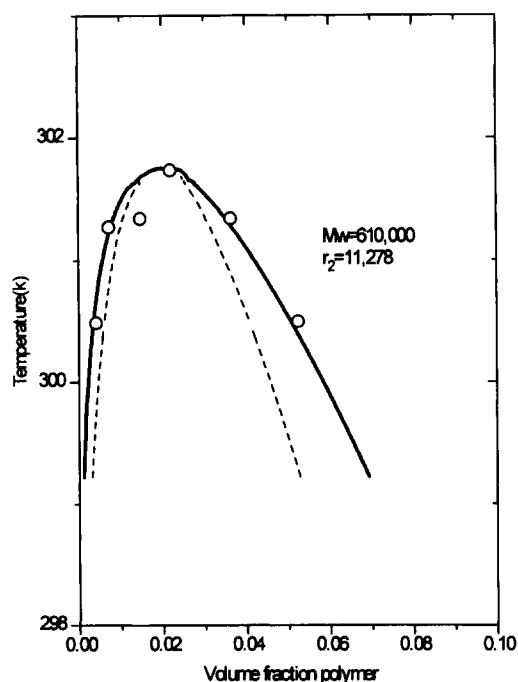


Figure 6 Coexistence curves for the PS/cyclohexane system. Open squares and circles are experimental data (Patterson and Delmas³²) for PS of molecular weight 610 000. The solid line is calculated by equations (17) and (18) (Case I). The dotted line is calculated using Case II

system. The ϵ/k value of Case II for PS of molecular weight 610 000 is 63.75 K. That of Case I is 74.19 K. The system is well known for having the specific interaction; however, Case I still gives very good agreement with experimental data.

In our proposed model (Case I), various flexibilities of chain molecules are not included. The model implicitly assumes that PIB (Figure 4) has the same flexibility as that of PS (Figures 5 and 6). Further, solvent molecules (diisobutyl ketone in Figure 4, cyclohexane in Figure 6, and *tert*-butyl acetate in Figure 5) are considered to be monomers where the concept of flexibility does not apply. It is likely that this deficiency is basically responsible for the discrepancy between our proposed model (Case I) and the experimental results.

CONCLUSIONS

The simplified and improved expression of $\Delta_{\text{mix}}U$ is proposed for the Helmholtz energy of mixing for monomer/*r*-mer mixtures obtained by correlating Monte-Carlo simulation results. For some binary systems, our correlating equation successfully predicts liquid-liquid equilibria for various molecular weights of polymers which takes into account the chain length dependence term. Our proposed

model (Case I) agrees remarkably well with experimental results.

ACKNOWLEDGEMENTS

This paper was supported by the Non-directed Research Fund, Korea Research Foundation, 1996. The authors are grateful to Dr S. M. Lambert for providing his simulation data.

REFERENCES

1. Chang, B. H. and Bae, Y. C., *Polymer*, (in press).
2. Redlich, O., Kister, A. T. and Turnquist, C. E., *Chem. Eng. Prog., Symp. Ser. No. 2*, 1952, **48**, 49-61.
3. Sanchez, C. and Lacombe, R. H., *J. Phys. Chem.*, 1976, **21**, 2352, 2568.
4. Sanchez, C. and Lacombe, R. H., *Macromolecules*, 1978, **11**, 1145.
5. Sanchez, C. and Balazs, A. C., *Macromolecules*, 1989, **22**, 2325.
6. Jang, J. G. and Bae, Y. C., *Macromolecules*, (submitted).
7. Flory, P. J., *J. Chem. Phys.*, 1942, **10**, 51.
8. Flory, P. J., *Principles of Polymer Chemistry*, Cornell University Press, Ithaca, 1953.
9. Flory, P. J., *J. Am. Chem. Soc.*, 1965, **87**, 1833.
10. Flory, P. J., *Discuss. Faraday Soc.*, 1970, **49**, 7.
11. Huggins, L., *J. Phys. Chem.*, 1942, **46**, 151.
12. Guggenheim, E. A., *Mixtures*, Clarendon Press, Oxford, Chapters 4, 10, and 11.
13. Dudowicz, J. and Freed, K. F., *Macromolecules*, 1990, **23**, 1519-1526.
14. Dudowicz, J. and Freed, K. F., *Macromolecules*, 1991, **24**, 5076-5095.
15. Dudowicz, J. and Freed, K. F., *Macromolecules*, 1991, **24**, 5096-5111.
16. Dudowicz, J. and Freed, K. F., *Macromolecules*, 1991, **24**, 5112-5123.
17. Dudowicz, J. and Freed, K. F., *Theor. Chim. Acta*, 1992, **82**, 357-382.
18. Freed, K. F., *J. Phys. A: Math. Gen.*, 1985, **18**, 871.
19. Madden, W. G., Pesci, A. I. and Freed, K. F., *Macromolecules*, 1990, **23**, 1181-1191.
20. Pesci, A. I. and Freed, K. F., *J. Chem. Phys.*, 1989, **90**, 2017-2026.
21. Lambert, S. M., Soane, D. S. and Prausnitz, J. M., *Fluid Phase Equilibria*, 1993, **83**, 59-68.
22. Bae, Y. C., *J. Ind. Eng. Chem.*, 1995, **1**, 18-27.
23. Hino, T., Lambert, S. M., Soane, D. S. and Prausnitz, J. M., *AIChE J.*, 1993, **39**, 5.
24. Qian, C., Mumby, S. J. and Eichinger, B. E., *Macromolecules*, 1991, **24**, 1655.
25. Hu, Y., Lambert, S. M., Soane, D. S. and Prausnitz, J. M., *Macromolecules*, 1991, **24**, 4356.
26. Flory, P. J. and Shultz, A. R., *J. Am. Chem. Soc.*, 1952, **74**, 4760.
27. Hu, H. L., Soane, D. S. and Prausnitz, J. M., *Fluid Phase Equilibria*, 1991, **67**, 65.
28. Oh, J. S. and Bae, Y. C., *Polymer*, (submitted).
29. Kurata, *Thermodynamics of Polymer Solutions*, Harwood Academic, NY, 1982.
30. Bae, Y. C., Lambert, S. M., Soane, D. S. and Prausnitz, J. M., *Macromolecules*, 1991, **24**, 4403.
31. Bae, Y. C., Shim, J. J., Soane, D. S. and Prausnitz, J. M., *J. Appl. Polym. Sci.*, 1993, **47**, 1193.
32. Patterson, D. and Delmas, G., *Trans. Faraday Soc.*, 1969, **65**, 708.